

Synthesis of GaN/ZnO heterostructure thin film on silicon substrate by pulsed laser deposition for ammonia detection

ZENA E. SLAIBY*, ASMIET RAMIZY

Physics Department, University of Anbar, College of Sciences, Anbar, Iraq

GaN/ZnO nano-heterostructure ZnO and GaN nanofilms were grown on a silicon Si(111) substrate prepared through pulse laser deposition technique for ammonia (NH₃) gas sensors. The structures of the GaN and ZnO layers were visualized using a field emission scanning electron microscope. The surface morphology of the thin GaN and ZnO nanofilms were characterized through atomic force microscopy. The films were extremely dense and have a smooth surface morphology. X-ray diffraction patterns showed crystallized hexagonal structures. The elemental compositions of the thin GaN and ZnO films were identified through energy dispersive X-ray analysis. The GaN/ZnO/Si composite exhibited excellent response as an ammonia gas sensor. The gas sensitivity of the gas sensor device for NH₃ gas were measured as a function of concentration. Device sensitivity increased from 32.0904% to 50.08441%, and gas concentration increased from 500 ppm to 1500 ppm.

(Received January 13, 2020; accepted October 22, 2020)

Keywords: GaN/ZnO, Pulsed laser deposition, NH₃ gas sensor

1. Introduction

Nitride semiconductors (III-N) have been subject to extensive research because of their unique properties, such as direct band gap and high chemical, mechanical, and thermal stability, which make them an excellent choice for the development of electronic, optoelectronic, and spintronic devices. Additionally, these semiconductors have wurtzite crystal structures. GaN has a wide direct energy band gap (3.4 eV) and is thus an ideal candidate for many applications, such as laser diodes, light-emitting diodes, UV detectors, and solar cells. It is a promising material for sensors operated in harsh environments [1-4]. Currently, the use of sensors in developing environmental and safety monitoring devices for gases has attracted considerable interest, and the sensors that optimize combustion reactions has become an important necessity in emerging transportation industries and industrial and domestic applications. The adsorption of gas molecules on semiconductor surfaces can significantly change the electrical resistance of materials [5]. GaN growth on Si substrates is one of the most interesting issues because GaN has many advantages, such as low cost, large area, and good electrical and thermal conductivity. However, the high-quality epitaxial growth of GaN on Si substrates is restricted by variations in thermal expansion coefficients and large mismatch between GaN and Si lattices [6]. The buffer layer of ZnO may have some advantages because ZnO shows only a 1.8% lattice mismatch with GaN and ZnO and can grow on different substrates [7]. ZnO is considered a promising substrate for GaN films owing to the following reasons: it has the same wurtzite structure

[8]; it is one of most important semiconductors, which has attracted considerable attention because of its unique material characteristics, such as a large excitation binding energy of 60 meV and wide band gap of 3.37 eV [5]; it is nontoxic [9]; and it has a high photoconductivity and is easy to fabricate, a low cost compound, and sensitive to the UV region. This properties make ZnO a suitable photonic material for several applications, such as UV detectors, light-emitting diodes, gas sensors, and transparent conducting electrodes [10]. Recently, ZnO has been grown on GaN through magnetron sputtering, metal organic chemical vapor deposition, molecular beam epitaxy, and pulse laser deposition [11].

The pulse laser deposition (PLD) technique is suitable for growing high-quality films at a low Ts [12]. PLD is interesting because it enables the on-site processing of multilayer structures by using multiple targets, provides flexible doping options for complex compositions, and enables stoichiometric transfer deposition from target to substrate [13]. In this work, a gas sensor device was synthesized using a thin film with GaN/ZnO/Si heterostructure through pulsed laser deposition, and the sensitivity of the fabricated device for ammonia detection was studied.

2. Experimental part

ZnO films were grown on an unheated n-type Si(111) substrate through a simple technique (PLD), as shown in Fig. 2 [14]. The deposition of the film was carried out inside a vacuum chamber, which was evacuated to a

pressure of 1×10^{-1} mbar. An Nd:YAG laser (Huafei Tongda Technology-Diamond-288 pattern EPLS) with a wavelength 1064 nm (500 pulses, repetition of 6 Hz and energy of 100 MJ) was focused on the ZnO target. The sample was annealed at 400 °C for 30 min. The GaN film was deposited on Si and ZnO/Si substrates under a nitrogen atmosphere, and the film was deposited through the same technique at 1×10^{-1} mbar, 300 pulses, repetition of 6 Hz, and energy of 300 MJ. The sample was annealed in a furnace, and N_2 was introduced to the tube. After the furnace reached a temperature of 700 °C, NH_3 was introduced. After the furnace reached a temperature of 900 °C for 2 h, the sample was taken out to cool down for subsequent characterization. The targets used for PLD were prepared by pressing corresponding compounds in their powder forms. ZnO and GaN in powder form were obtained from the Sigma-Aldrich Company. For the fabrication of the gas sensor, a silver (Ag) metal contact was deposited on the GaN/ZnO/Si surface with a vacuum evaporation system, as shown in Fig. 3 [15].

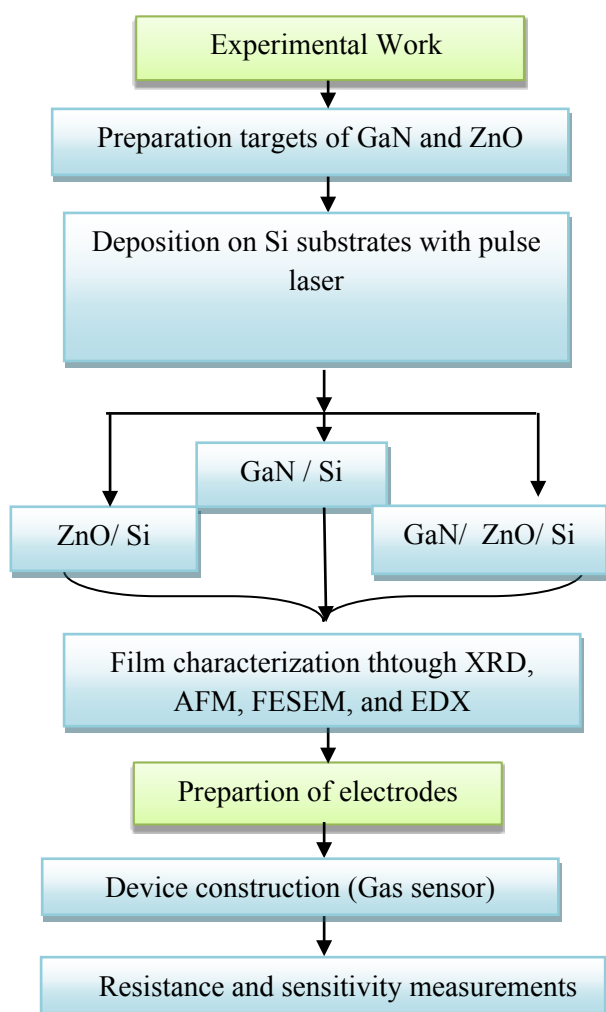


Fig. 1. Experimental setup (color online)

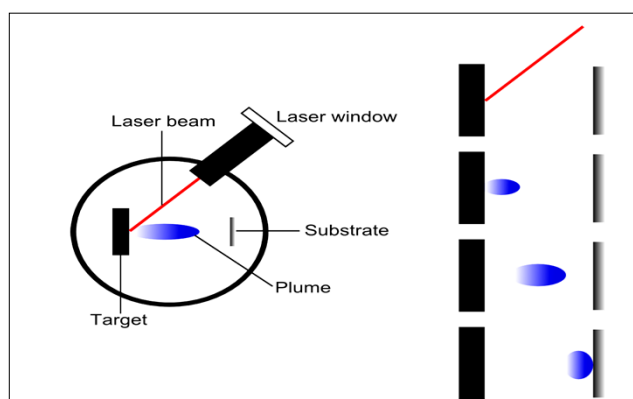


Fig. 2. Schematic of the PLD process (color online)

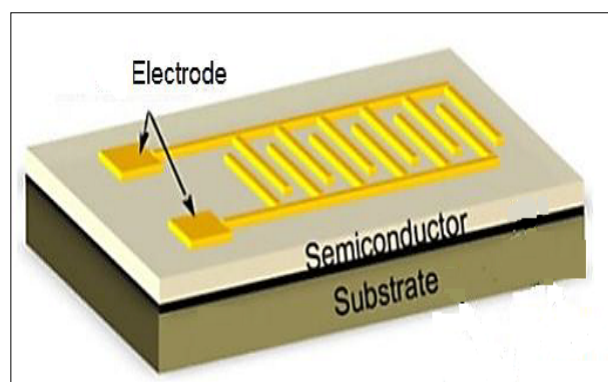


Fig. 3. Shape of the contact (color online)

3. Results and discussion

3.1. X-ray diffraction analysis

The typical X-ray diffraction (XRD) patterns of the ZnO and GaN films and GaN/ZnO deposited on Si (111) through PLD are shown in Fig. 4 (a), (b), and (c), respectively. The spectrum revealed a number of peaks for ZnO on Si, a strong peak at 28.447° for Si (111), and diffraction peaks corresponding to the (002), (012), (110), (013), (020), (112), and (022) planes of the ZnO structure located at 33.504°, 47.544°, 56.519°, 62.859°, 66.396°, 67.961°, and 76.977°, respectively, which was found to well matched with wurtzite structure of ZnO that having hexagonal phase and good agreement with relevant XRD database standard JCPDS (card No. 98-004-1488). The strong intensities and narrow widths of the ZnO diffraction peaks indicated that the products have good crystalline structures [16]. Fig. 4 (b) shows the the peaks for GaN on the Si substrate. The strong peak at 28.6273° was from the silicon substrate Si(111), and the peak at 32.639° was from GaN (100). The peak at 64.2711° corresponded to GaN (013). GaN showed a hexagonal phase according to the PDF (00-050-0792) card. Fig. 4 (c) shows that peaks for GaN/ZnO deposited on the Si substrate. The peak corresponded to the (400) plane of Si at 25.6968°, and the

strong peak at 28.5109° was attributed to Si (111). The peak with a low intensity appeared at a diffraction angle (2 theta) of 35.8009° and may be attributed to $\text{Ga}_1\text{O}_4\text{Zn}_3(150)$, which have an orthorhombic phase according to JCPDS (card No. 98-026-0746). However,

this compound may have formed because of the high preparation energy of the materials. Another peak at 58.8984° corresponded to the GaN(013) plane. GaN showed a hexagonal phase, and this structure showed good agreement with JCPDS (card No. 98-004-2000).

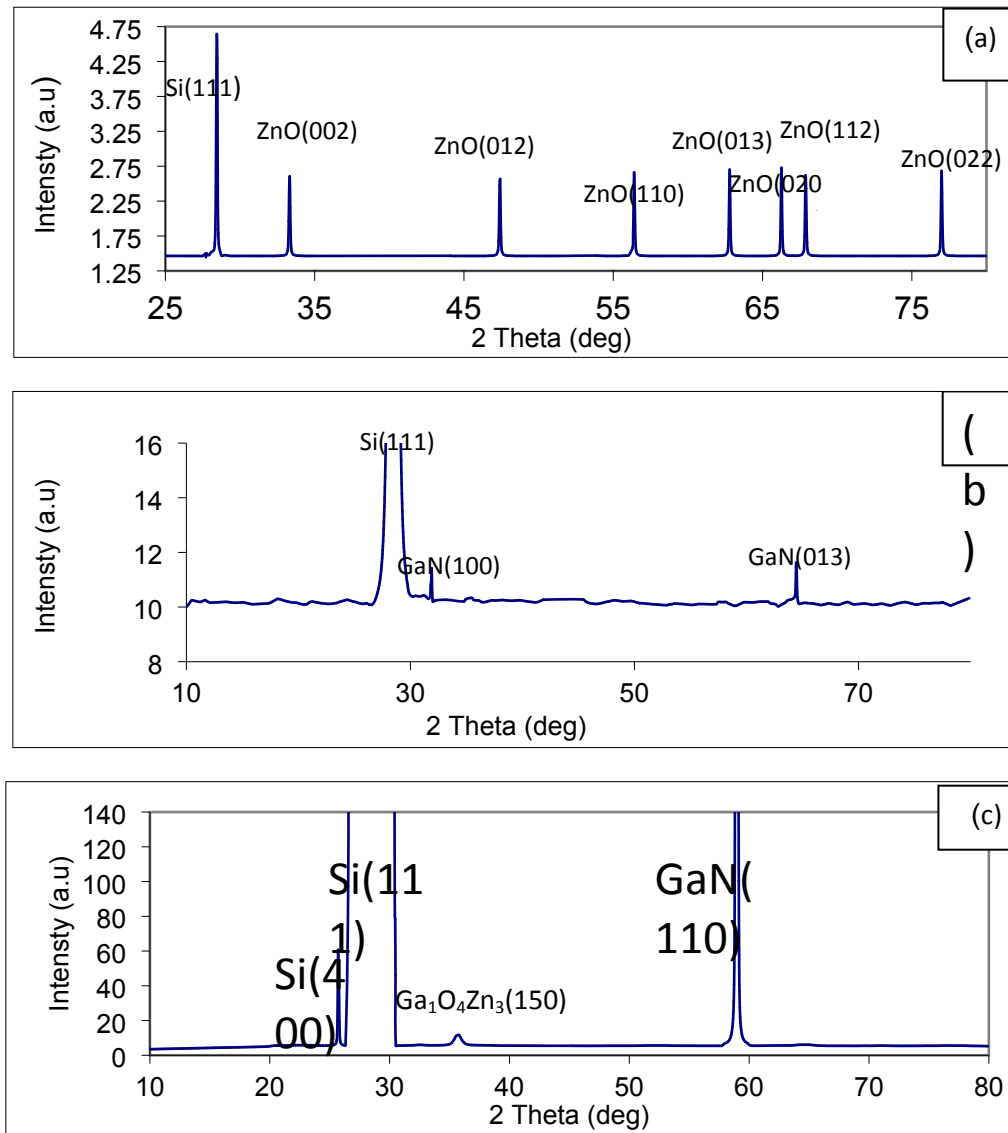


Fig. 4. X-ray diffraction of (a) ZnO/Si, (b) GaN/Si, and (c) GaN/ZnO/Si (color online)

3.2. AFM analysis

The surface morphology and surface roughness of the films were studied using the AFM technique. Fig. 5 (a) shows the 3-D and 2-D AFM images of the thin ZnO nanofilm. The nanofilm was extremely dense and showed a smooth surface morphology. The average roughness and root-mean square for the sample was determined. The roughness analysis results obtained through AFM showed that the average surface roughness (S_a) was 5.86 nm and root mean square was 6.77 nm, which are in a good

agreement with the results of previous reports [17-19]. Fig. 5 (b) shows the 3-D and 2-D AFM images of the GaN film with an average roughness of 7.4 nm and root mean square of 8.55 nm. Fig. 5 (c) shows the 3-D and 2-D AFM images of the GaN/ZnO film with an average roughness of 24.948 nm, root mean square of 32.219 nm, and a high-quality crystal structure, showing that the crystalline quality of the GaN film was high in the ZnO buffer layers. GaN film deposited on the crystalline ZnO buffer layer had a smooth surface, as shown in Fig. 5 (c) [20].

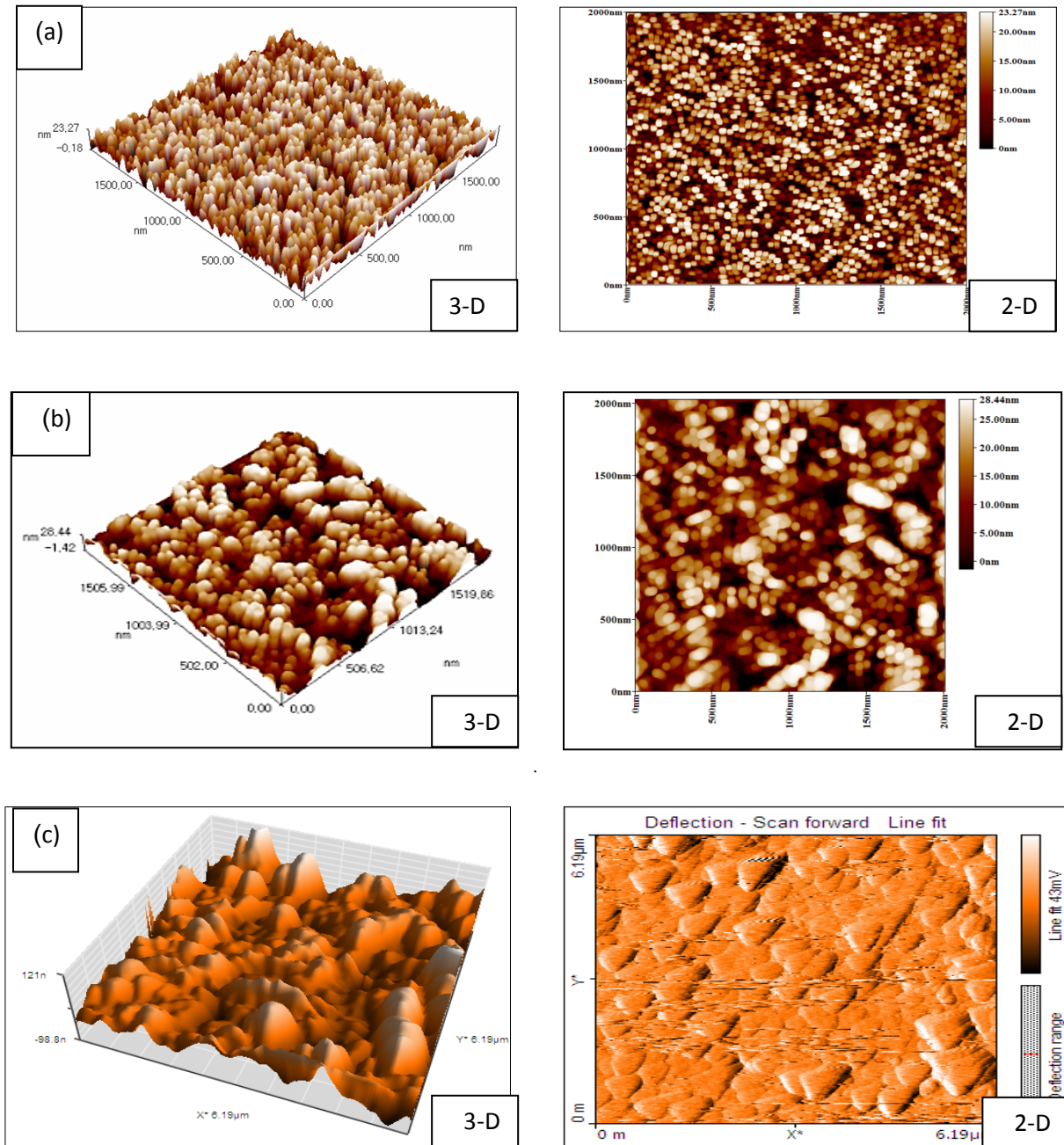


Fig. 5. (a) AFM images of ZnO/Si film, (b) AFM images of GaN/Si film, and (c) AFM images of the GaN/ZnO/Si film (color online)

3.3. Field emission scanning electron microscopy analysis

The field emission scanning electron microscopy (FESEM) images of the thin ZnO, GaN, and GaN/ZnO films deposited on Si substrates are shown in Fig. 3. Fig. 6 (a) shows that the ZnO nanoparticles had a compact and uniform arrangement and nearly irregular shapes. The particles varied in size in the prepared sample. The large particles in the sample were composed of small crystallites [21]. Fig. 6 (b) and (c) show the presence of many GaN grains with uniform sizes on the film surface. The reason

was that energy was sufficient to move adsorbed atoms on the surface of GaN film to the lowest energy point at a high temperature. This condition led the uniform grain size and dense structure of the film at the macro level. Fig. 6 (c) shows that Si-based GaN films prepared with ZnO as a buffer layer have a fine crystallization quality at an annealing temperature of 900 °C [22]. The smooth surface morphology was achieved by introducing a GaN layer onto the ZnO buffered substrate. This finding supports the important role of ZnO as a buffer layer [23].

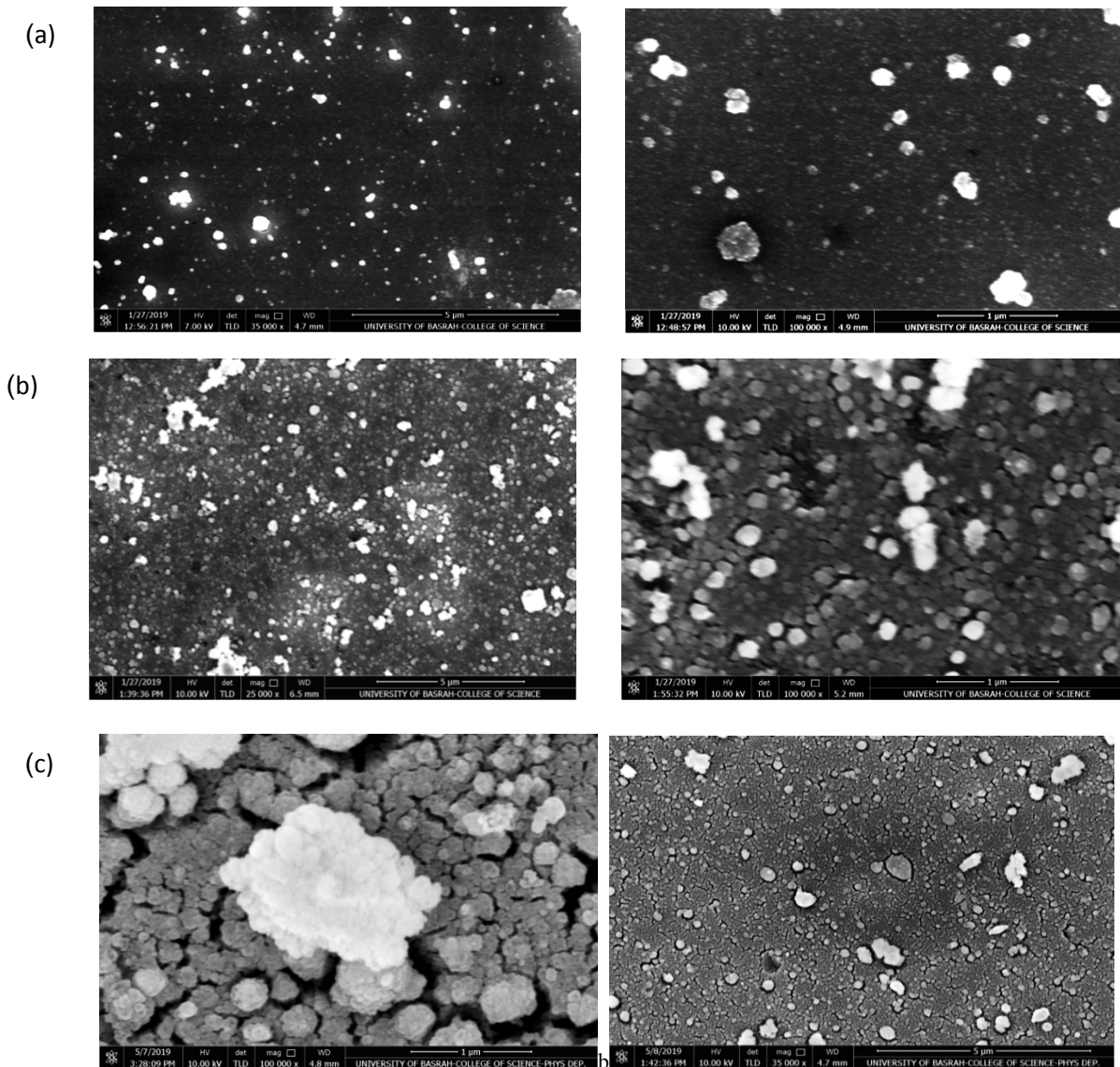


Fig. 6(a). Grains observed by use FESEM analysis for ZnO /Si, (b). Grains observed by use FESEM analysis for GaN /Si and (c). Grains observed by use FESEM analysis for GaN/ ZnO /Si

3.4. Energy dispersive X-ray analysis

The chemical composition of the ZnO, GaN, and GaN/ZnO films were confirmed through energy dispersive X-ray (EDX) analysis, as shown in Fig. 7. Fig. 7 (a) shows that Zn, O, and Si elements constituted the ZnO thin film. The compositional analysis of the EDX spectrum refers to the atomic ratio for O that is larger than Zn in the ZnO film. Specifically, the ZnO film had an excessive amount of oxygen may be from oxygen ions on the surface. This finding is in agreement with the findings in [18]. Fig. 7 (b)

shows that Si, N, and Ga from the substrate and GaN layer contained oxygen impurities, as indicated by the EDX analysis results, which may have been introduced by air leakage [24]. The EDX spectrum in Fig. 7 (c) shows the existence of O and Zn peaks representing the ZnO nanostructure determined through elementary characterization. The purity of the fabricated films was excellent, which had no residues (except Si, Ga, and N derived from the substrate and GaN layer). This result is in good agreement with the results in [11].

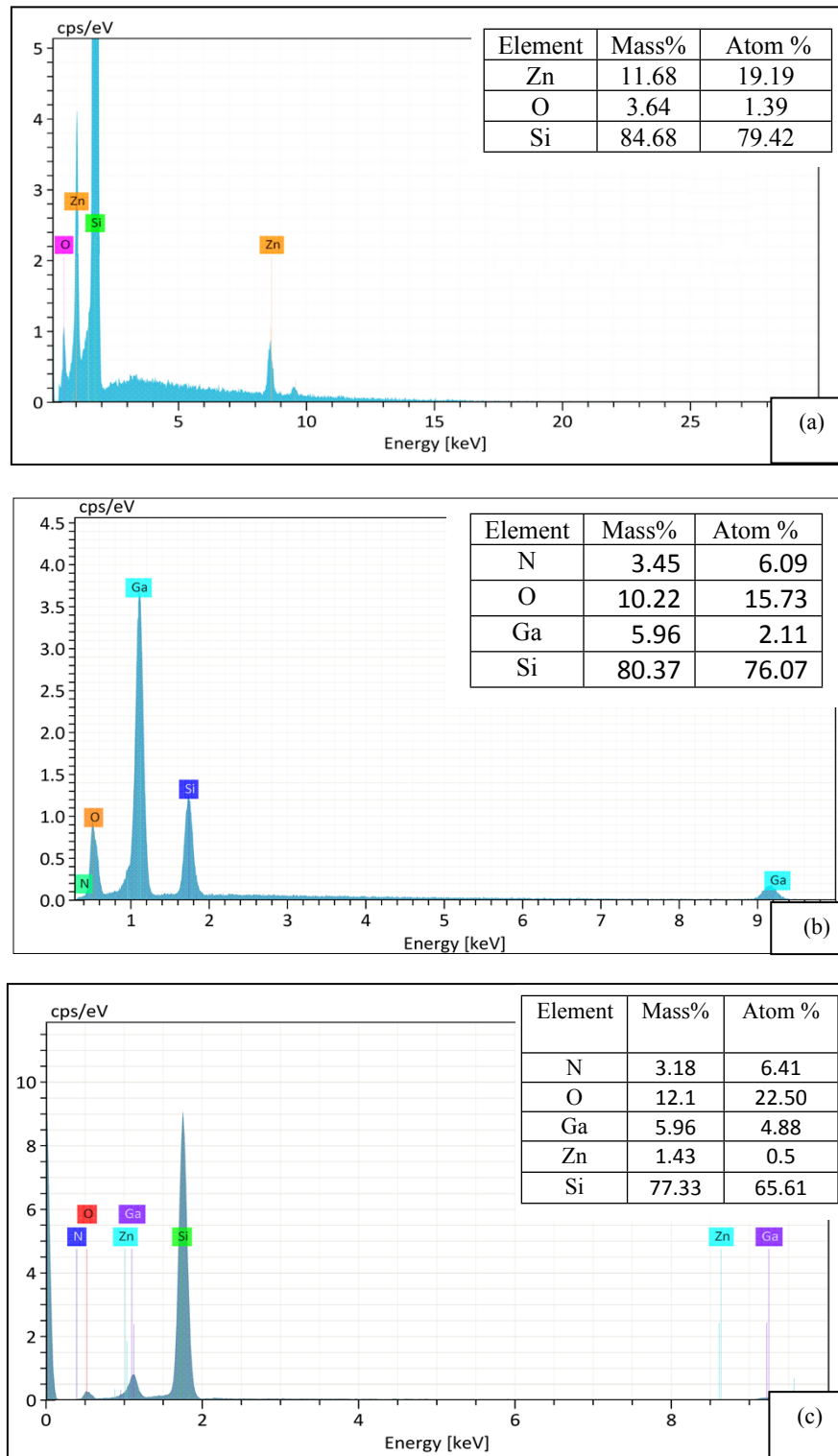


Fig. 7. EDX analyses of films prepared by pulse laser deposition (a) ZnO/Si, (b) GaN/Si, (c) GaN/ZnO/Si (color online)

3.5. Gas sensor measurement

The semiconductor nanostructures of nitride and oxide materials are ideal for chemical sensing. The material properties, including high thermal, chemical stability, and high surface-to-volume ratio, afford nanostructured

sensors high sensitivity and detection capabilities at low gas concentration [25]. The gases sensitivity S is defined as

$$S = (R_o - R_{gs})/R_o \quad (1)$$

where R_0 is the resistance of sensors before gas passage and R_{gs} is the resistance after gas passage [26]. The interactions of the gas/semiconductor surface based on the gas-sensing mechanism of semiconductor gas sensor occurred at the grain boundaries of the films. These interactions included the reduction/oxidation processes of the semiconductor and the adsorption of chemical species directly on the semiconductor. The effect of these surface phenomena changed with electrical resistance. Variations in resistance were easily observed and used in detecting chemical species under ambient conditions [27]. Fig. 8 shows the schematic diagram of the gas sensor setup [15].

Gas sensing under a constant temperature but varying gas concentrations was studied for thin GaN/ZnO films. Fig. 9 shows that resistance changed over time with concentration. Additionally, sensitivity increased with gas concentration, and the sensitivity of the gas sensor device to NH_3 gas was measured as a function of concentration, as shown in Fig. 10. The sensitivity of the device increased from 32.0904% to 50.08441%, and gas concentration increased from 500 ppm to 1500 ppm, respectively. Given that gas concentration may change rapidly, the sensors were expected to show a fast dynamic response with small changes in concentration [28].

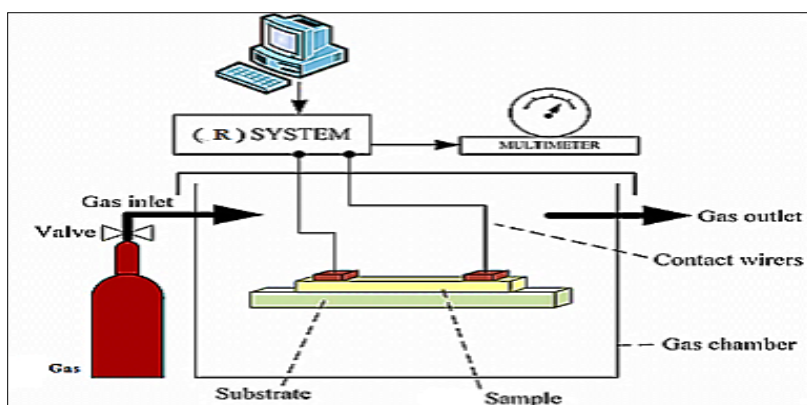


Fig. 8. Schematic diagram of the gas sensor setup (color online)

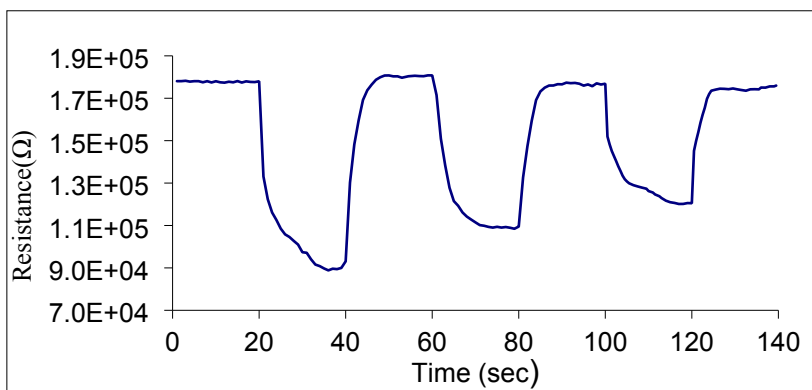


Fig. 9. Resistance changes over time (color online)

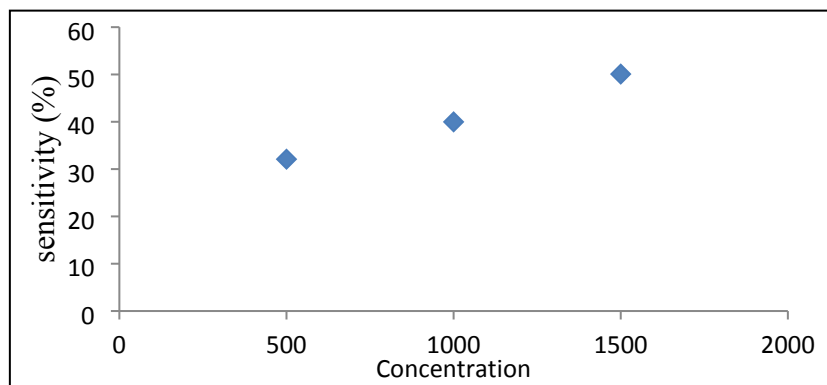


Fig. 10. Sensitivity over concentration of gas (color online)

4. Conclusion

High-quality ZnO, GaN, and GaN/ZnO films were fabricated through simple technique (PLD) on a Si substrate. The structures of the GaN and ZnO layers were visualized using FESEM and AFM. The film were extremely dense and showed a smooth surface morphology. The XRD patterns showed crystallized hexagonal structures. GaN/ZnO/Si exhibited excellent response as an ammonia gas sensor. The gas sensitivity of the gas sensor device for NH₃ gas was measured as a function of concentration. Device sensitivity increased from 32.0904% to 50.08441%, and gas concentration increased from 500 ppm to 1500 ppm.

References

- [1] Luis Alberto Hernandez-Hernandez, Jorge R. Aguilar-Hernandez, Francisco de Moure-Flores, Osvaldo de Melo-Pereira, Concepcion Mejia-Garcia, Francisco Cruz-Gandarilla, Gerardo Contreras-Puente, *Materials Research* **20**(6), 1707 (2017).
- [2] M. Baseer Haider, M. F. Al-Kuhaili, S. M. A. Durrani, Imran Bakhtiari, *J. Mater. Sci. Technol.* **29**(8), 752e756 (2013).
- [3] Ho Xin Jinga, Che Azuranim Che Abdullaha, Mohd Zaki Mohd Yusoffc, Azzafeerah Mahyuddind, Zainuriah Hassane, *Results in Physics* **12**, 1177 (2019).
- [4] Asmiet Ramizya, Issam M. Ibrahim, Maryam Th. Muhammed, *Optik* **126**, 3125 (2015).
- [5] H. S. Hassan, A. B. Kashyout, I. Morsi, A. A. A. Nasser, A. Raafat, *American Institute of Physics* **1653**, 020042 (2015).
- [6] M. Yang, H. S. Ahn, J. H. Chang, S. N. Yi, K. H. Kim, H. Kim, *Journal of the Korean Physical Society* **43**(6), 1090 (2003).
- [7] Hyoun Woo Kim, Nam Ho Kim, *Applied Surface Science* **236**, 192 (2004).
- [8] A. Ougazzaden, D. J. Rogers, F. Hosseini Teherani, T. Moudakir, S. Gautier, T. Aggerstam, S. Ould Saad, J. Martin, Z. Djebbour, O. Durand, G. Garry, A. Lusson, D. Mc Grouther, J. N. Chapman, *Journal of Crystal Growth* **310**, 947 (2008).
- [9] Boban Gavric, Investigation of ZnO nanorods for UV detection, Royal Institute of Technology (KTH) Functional Materials Division, School of ICT Electrum 229, Isafjordsgatan 22, SE-16 440 Stockholm, Sweden, 2011.
- [10] Hamza Hassan Hamza, Structural and Optical Properties of ZnO Thin Films Deposited on Poly Propylene Carbonate (PPC) Plastic Substrates By PLD, Al-Mustansiriyah University, (2015).
- [11] Xianqi Wei, Ranran Zhao, Minghui Shao, Xijin Xu, Jinzhao Huang, *Nanoscale Research Letters* **8**, 112 (2013).
- [12] T. Ohshima, R. K. Thareja, T. Ikegami, K. Ebihara, *Surface and Coatings Technology* **169–170**, 517 (2003).
- [13] Wei-Kai Wang, Shih-Yung Huang, Ming-Chien Jiang, Dong-Sing Wu, *Appl. Sci.* **7**, 87 (2017).
- [14] Carl Philip J Heimdal, Pulsed Laser Deposition of Zinc Sulfide Thin Films on Silicon, Norwegian University of Science and Technology, Department of Physics, 2014.
- [15] Abu Bakr Sabbar Mohammed, Synthesis and Characterization of Rare Earth Doped NiO Nanostructure on Si and PSi H₂S Sensor and Photo detector, University of Anbar, 2018.
- [16] Hind Ibraheem Abdulgafour, Hassan Hadi Darwoysh, Faez Mohamad Hassan, *Journal of Materials Science and Engineering A* **6**(3-4), 56 (2016).
- [17] Siti Huzaimah Ribut, Che Azuranim Che Abdullah, Mohd Zaki Mohammad Yusoff, *Results in Physics* **13**, 102146 (2019).
- [18] Peihong Wang, Hejun Du, Shengnan Shen, Mingsheng Zhang, Bo Liu, *Nanoscale Research Letters* **7**, 176 (2012).
- [19] Sara Marouf, Abdelkrim Beniaiche, Hocine Guessas, Amor Azizi, *Materials Research* **20**(1), 88 (2017).
- [20] B. Y. Man, C. Yang, H. Z. Zhuang, M. Liu, X. Q. Wei, H. C. Zhu, C. S. Xue, *Journal of Applied Physics* **101**, 093519 (2007).
- [21] Zhezhe Wang, Hongchao Shang, Rongjun Zhao, Xinxin Xing, Yude Wang, *J. Nanostruct.* **7**(2), 103 (2017).
- [22] Jianting He, Shulian Yang, Qinqin Wei, *Journal of Photonic Materials and Technology* **5**(1), 1 (2019).
- [23] R. P. Wang, H. Muto, Y. Yamada, T. Kusumori, *Thin Solid Films* **411**, 69 (2002).
- [24] M. Gholampour, A. Abdollah-Zadeh, R. Poursalehi, L. Shekari, S. Hatamikhah, *Procedia Materials Science* **11**, 300 (2015).
- [25] J. S. Wright, Wantae Lim, D. P. Norton, S. J. Pearton, F. Ren, Jason L. Johnson, *Ant Ural, Semicond. Sci. Technol.* **25**, 7 (2010).
- [26] Fawzy A. Mahmoud, G. Kiriakidis, *Journal of Ovonic Research* **5**(1), 19 (2009).
- [27] S. Capone, A. Forleo, L. Francioso, R. Rella, P. Siciliano, J. Spadavecchia, D. S. Presicce, A. M. Taurino, *J. Optoelectron. Adv. M.* **5**(5), 1335 (2003).
- [28] Yacine Halfaya, Chris Bishop, Ali Soltani, Suresh Sundaram, Vincent Aubry, Paul L. Voss, Jean-Paul Salvestrini, Abdallah Ougazzaden, *Sensors* **16**, 273 (2016).

*Corresponding author: asmat_hadithi@uoanbar.edu.iq